GANIT

Available online at https://ganitjournal.bdmathsociety.org/

GANIT: Journal of Bangladesh Mathematical Society

**GANIT** *J. Bangladesh Math. Soc.* 43.2 (2023) 49–64
DOI: https://doi.org/10.3329/ganit.v43i2.70798.

# Mathematical Model for Optimal Dubins Path to Intercept a Stationary Target

M. Akter [*a], M. M. Rizvi[b], and M. Forkan[a]

[a] *Department of Mathematics, University of Chittagong, Chittagong-4331, Bangladesh.*
[b] *Centre for Smart Analytics (CSA), Institute of Innovation, Science and Sustainability, Federation University Australia*

## ABSTRACT

This paper presents a comprehensive mathematical model designed to determine the most efficient trajectory for intercepting a stationary target, with a primary focus on minimizing interception time and resource utilization. The proposed model incorporates key parameters such as target location, interception speed, and environmental constraints to formulate a set of differential equations that describe the motion dynamics of both the pursuer and the target. The objective function is defined to optimize the interception path. The study employs advanced mathematical techniques, including optimal control theory and numerical optimization algorithms, to solve the formulated equations and derive the optimal path. The model is adaptable to various scenarios, accounting for different pursuit vehicle dynamics and target characteristics. Simulation results are presented to validate the effectiveness of the proposed mathematical model in practical applications.



**Received:** December 05, 2023 **Accepted:** December 27, 2023 **Published Online:** December 31, 2023

**Keywords:** Dubins path; Optimal control problem; Stationary target; Path planning; Numerical methods.

## 1 Introduction

Path planning is becoming more and more important as a result of the rapid improvements in technology that have led to an increase in the employment of autonomous air vehicles in both military and civilian contexts. We take into consideration an application in which a stationary target is pursued and intercepted by an autonomous aerial vehicle. This paper contributes to the field of path planning and interception strategies by providing a robust mathematical framework that can enhance the efficiency and effectiveness of systems designed for intercepting a stationary target. Dubins [1] presented the Dubins car model, which is a vehicle with a finite maximum turn rate and constant speed. He demonstrated that the minimum-time paths for these vehicles between two points can only be made up of curves (C) that have maximum-rate turns left (L) and right (R) and combinations of straight lines (S).There demonstrated the existence of such minimum-length paths and the necessity of their having the forms CSC, CCC, or reduced versions. Since then, Dubins findings have been expanded upon utilizing nonlinear optimal control theory, specifically Pontryagin's principle in ([2]-[7]) and geometry Ayala et al. [8]. Recently, researchers have looked into the challenge of determining a Dubins car's minimum-time path from a fixed location to any point on a circle with the final heading tangent to the circle

*Corresponding author. *E-mail address:* masuda@cu.ac.bd

([9]-[11]). A comprehensive discussion of optimal search for a stationary target can be found in [12]. In order to accomplish simultaneous target interception for a team of n pursuers, cooperative geometrical rules and matching guidance laws, were given and examined in [13]. The topic of optimally guiding an interceptor to a stationary target in a nonlinear environment is studied in [14]. In [15] a algorithms for nonlinear estimating and optimal guidance are developed to intercept a stationary target vehicle that has been slowed down by atmospheric drag. The simultaneous attack problem of many missiles against a stationary target is examined in [16].

Furthermore, Looker [17] proposes a search algorithm for determining the shortest CS type path to interception under the assumptions of a pursuer modeled as a Dubins vehicle and of a constant velocity target. Yalcin Kaya [18] reformulated the Markov-Dubins problem as an optimal control problem while identifying the many forms of shortest bounded curves that connect two oriented points. Later, the author have extended his work as the Markov- Dubins interpolation problem, where the problem is also considered as an optimal control problem and obtain the solution by applying optimal control theory [19]. Zheng [20] was presented with an idea involving a Minimum-Time Intercept Problem (MTIP), in which a Dubins vehicle is led to intercept a moving object in the shortest amount of time by starting from a place with a predetermined initial heading angle. More recently, Forkan et al. [21] introduced an innovative mathematical model to find a minimum path length or minimum time for touring a finite number of targets by unmanned aerial vehicle (UAV), both the UAV and targets are at the same altitude. The authors are used arc parameterization technique to determine the optimal path. To approximate the optimal path for the pursuer to intercept a stationary target, this study is presented through a geometric interpretation and a mathematical model that is demonstrated in Sections 3 and 4.

In this paper, we present a novel algorithm that makes a significant contribution to generating efficient paths for pursuers. We formulate mathematical expressions based on geometric principles and subsequently devise new algorithms aimed at approximating pursuer paths for intercepting stationary targets. Our objective is to compute feasible paths and determine the most optimal trajectory for pursuers, ultimately optimizing their paths to intercept the target.

The subsequent sections make up the remainder of this paper. In Section 2 we demonstrate how to reframe the Dubins problem in the scenario of time-optimal control. Later we state the Pontryagin's Maximum Principle for pursuers length functional. A pursuers best path planning for intercepting a stationary target is explained geometrically in Section 3. The model for determining the pursuers optimal route to intercept a stationary target is presented in Section 4. We present an algorithm in Section 5 to carry out the suggested model. In Section 6, we present the findings and discussions derived from computational tests that are executed. Presenting the paper's conclusion is the final phase.

## 2 Formulation of Optimal Control Problem and Pontryagin's Maximum Principle

In this section, we formulate the optimal control problem for the intercepting the stationary target by pursuer and then utilize the Pontryagin's Maximum Principle [22] to analyze control law. Assuming that $\ell(t) : [t_0, t_f] \to \mathbb{R}^2$ be the optimum path of interception. We also assume that the pursuer move only the forward direction through the Dubins path. Let the kinemetic equations of the pursuers path be

$$\begin{bmatrix} \dot{x}(t) \\ \dot{y}(t) \\ \dot{\theta}(t) \end{bmatrix} = \begin{bmatrix} \cos\theta(t) \\ \sin\theta(t) \\ u(t) \end{bmatrix}$$

where $\theta(t)$ denotes the heading angle of the pursuer, which is measured with $\theta(t) \in [0, 2\pi]$ and counterclockwise from the $x$-axis. It is also considered that the pursuer moves with the unit turning radius of its turning circle with unit velocity. In order to intercept a stationary target, the pursuer's minimum path is determined by the arc length functional as below.

$$\int_{t_0}^{t_f} \sqrt{\dot{x}^2 + \dot{y}^2}\, dt = \int_{t_0}^{t_f} ||\dot{\ell}(t)||\, dt = (t_f - t_0), \tag{2.1}$$

The curvature at each point along the path is determined by $b = |\dot{\theta}(t)|$. The sign of the quantity $\dot{\theta}(t)$ indicates whether it is positive or negative. When $\dot{\theta}(t) > 0$, the pursuer turns left $(L)$ i.e. proceeds counterclockwise. Additionally, if $\dot{\theta}(t) < 0$, the pursuer goes in a clockwise direction (making turns right $(R)$) and also the pursuer

moves in a straight line $(S)$ if $\dot{\theta}(t) = 0$. Here, the control variable is defined as $u(t) = \dot{\theta}(t)$. Let us consider that the pursuers initial location is $P(x_0^P, y_0^P)$ with heading angles at $\theta_0^P$. Hence the optimal control problem for the pursuer can be formulated as follows,

$$\begin{aligned} \min \quad & f = \int_{t_0}^{t_f} dt = (t_f - t_0). \\ \text{subject to} \quad & \\ & \dot{x}^P(t) = \cos\theta^P(t),\ x^P(t_0) = x_0^P, x^P(t_f) = x_f^P \\ & \dot{y}^P(t) = \sin\theta^P(t),\ y^P(t_0) = y_0^P, y^P(t_f) = y_f^P \\ & \dot{\theta}^P(t) = u(t),\ \theta^P(t_0) = \theta_0^P \\ & |u(t)| \leq b. \end{aligned} \tag{2.2}$$

## 2.1 Pontryagin's Maximum Principle

The essential conditions of optimality under Pontryagin's maximum principle [22] for Problem (2.2) will be stated in this subsection in order to determine the best path for a pursuer to intercept a stationar target.
Now set up the following definition of the Hamiltonian function for the problem (2.2).

$$\begin{aligned} H(x^P(t), y^P(t), \theta^P(t), \nu_0, \nu_1(t), \nu_2(t), \nu_3(t), u(t)) = \\ \nu_0 + \nu_1(t)\cos\theta^P(t) + \nu_2(t)\sin\theta^P(t) + \nu_3(t)\,u(t)\,, \end{aligned} \tag{2.3}$$

where $\nu_0$ is a scalar parameter and $\nu_i : [t_0, t_f] \in \mathbb{R}, i = 1, 2, 3$, are the costate variables.
The costate variables are required to satisfy

$$\dot{\nu}_1(t) = -H_{x^P}(t) = 0, \tag{2.4}$$

$$\dot{\nu}_2(t) = -H_{y^P}(t) = 0, \tag{2.5}$$

$$\dot{\nu}_3(t) = -H_{\theta^P}(t) = \nu_1(t)\,\sin\theta^P(t) - \nu_2(t)\,\cos\theta^P(t). \tag{2.6}$$

In addition to (2.4)-(2.6), there are state differential relations $\dot{x}^P(t) = H_{\nu_1}(t)$, $\dot{y}^P(t) = H_{\nu_2}(t)$, $\dot{\theta}^P(t) = H_{\nu_3}(t)$.
From (2.4) and (2.5), we have $\nu_1(t) = \bar{\nu}_1$, $\nu_2(t) = \bar{\nu}_2$ for all $t \in [t_0, t_f]$, where $\bar{\nu}_1$ and $\bar{\nu}_2$ are constants.
Suppose,

$$\nu_1(t) = \bar{\nu}_1 = \rho\cos\phi \tag{2.7}$$

$$\nu_2(t) = \bar{\nu}_2 = \rho\sin\phi \tag{2.8}$$

Now squaring and adding (2.7) and (2.8) we get,

$$\bar{\nu}_1^2 + \bar{\nu}_2^2 = \rho^2\cos^2\phi + \rho^2\sin^2\phi,$$

Therefore, $\rho = \sqrt{\bar{\nu}_1^2 + \bar{\nu}_2^2}$ and $\tan\phi = \dfrac{\bar{\nu}_2}{\bar{\nu}_1}$.
Using (2.7) and (2.8) we can rewrite the equation (2.3), we get,

$$H = \nu_0 + \rho\cos\phi\cos\theta^P(t) + \rho\sin\phi\sin\theta^P(t) + \nu_3(t)\,u(t)\,,$$

which implies,

$$H = \nu_0 + \rho\cos(\theta^P(t) - \phi) + \nu_3(t)\,u(t) \tag{2.9}$$

Using (2.7) and (2.8) we can rewrite the equation (2.6), we get,

$$\dot{\nu}_3(t) = \rho\cos\phi\sin\theta^P(t) - \rho\sin\phi\cos\theta^P(t),$$

which implies,

$$\dot{\nu}_3(t) = \rho\sin(\theta^P(t) - \phi) \tag{2.10}$$

The following criteria are met in addition to the state differential equations and other restrictions provided in (2.2), as well as the adjoint differential equations (2.4), (2.5), and (2.10):

$$u(t) \in \underset{||w|| \leq b}{arg\,min}\; H(x^P(t), y^P(t), \theta^P(t), \nu_0, \nu_1(t), \nu_2(t), \nu_3(t), w), \tag{2.11}$$

$$H(t) = 0. \tag{2.12}$$

Thus, using (2.3), equation (2.11) can be written more simply as,

$$u(t) \in \underset{||w|| \leq b}{arg\,min}\;\; \nu_3(t) w, \tag{2.13}$$

therefore minimizing the Hamiltonian function yields the following control law.

$$u(t) = \begin{cases} b, & \text{if } \nu_3(t) < 0 \\ -b, & \text{if } \nu_3(t) > 0 \\ \text{undetermined}, & \text{if } \nu_3(t) = 0. \end{cases} \tag{2.14}$$

Now from the equation (2.9) and (2.12) we can write the following equation,

$$\nu_0 + \rho \cos(\theta^P(t) - \phi) + \nu_3(t)\, u(t) \;= 0 \tag{2.15}$$

# 3 Geometrical Representation of the Interception of a Stationary Target

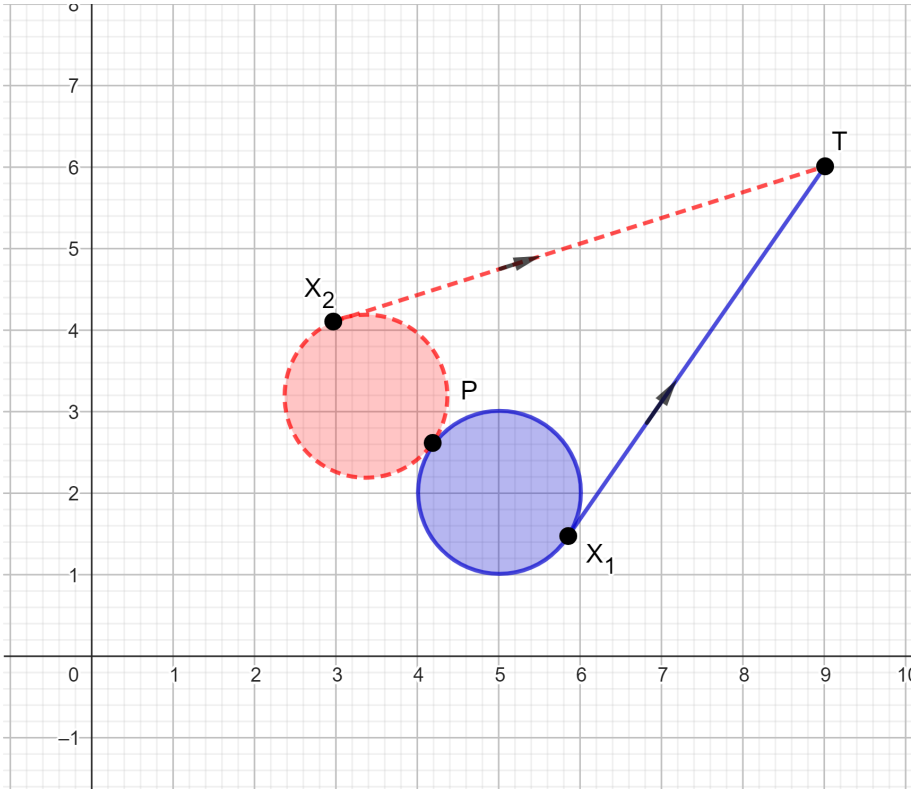


Figure 3.1: Feasible optimal paths of interception of a stationary target and a pursuer.

This section shows the optimal path planning for a pursuer to intercept a stationary target in two dimensions. The following illustrates the geometric interpretation for constructing a pursuers possible paths to intercept a stationary target. Let the pursuer start its journey with unit velocity from the points $P(x_0^P, y_0^P, \theta_0^P)$ and

the position of the stationary target is $T(x^T, y^T)$ and the pursuer eventually crosses the target after a specific period. The pursuer may turn left or right to optimize its trajectory by adhering to a minimum turning radius while following Dubins path. Figure (3.1) shows that the pursuer can move through a circular trajectory by taking either path $PX_1$ or $PX_2$. Then, depending on the orientation in which it turns, the pursuer proceeds in a straight line, either $X_1X_3$ or $X_2X_3$, in an attempt to intersect the target. Since the pursuer and the target coincide at the interception point *i.e* $X_3 = T$. This generates two probable pathways of type $CS$ which are as follows:

$$CS \equiv \begin{cases} LS \equiv \text{arc } PX_1 + \text{st. line } X_1X_3 & \text{or,} \\ RS \equiv \text{arc } PX_2 + \text{st. line } X_2X_3, \end{cases} \tag{3.1}$$

# 4 Mathematical Model for Intercepting a Stationary Target

In this section, we propose a mathematical model that shows how to find the most optimal path for a pursuer to take in order to intercept a stationary target. We present mathematical expressions to compute the concatenated lengths in accordance with the geometrical interpretation presented in Section 3. The sub-path $CS$ types are composed of these lengths. Moreover, the most appropriate plan for proceeding to intercept a stationary target belongs to one of the two special situations described in the set addressed in (3.1) below.

$$\{LS, RS\}\,. \tag{4.1}$$

Assuming that the pursuer has an initial time of $t_0 = 0$ and a final time of $t_f = t_3$, we may define the length of each sub-path as $\zeta_i = t_i - t_{i-1}$, for $i = 1, 2, 3$, and the time at which the pursuer intercepts it as $t_f = t_3$. Now we solve the ordinary differential equations given in (2.2) for $x^P(t)$, $y^P(t)$, $\theta^P(t)$ with the interval $t_{i-1} \le t \le t_i$, $i = 1, 2, 3$ yields,

$$\begin{aligned} \int_{t_{i-1}}^{t_i} \dot{x}^P(t)\,dt &= \int_{t_{i-1}}^{t_i} \cos\theta^P(t)\,dt, \\ \int_{t_{i-1}}^{t_i} \dot{y}^P(t)\,dt &= \int_{t_{i-1}}^{t_i} \sin\theta^P(t)\,dt, \\ \int_{t_{i-1}}^{t_i} \dot{\theta}^P(t)\,dt &= \int_{t_{i-1}}^{t_i} u(t)\,dt. \end{aligned} \tag{4.2}$$

The location $(x^P(t_i), y^P(t_i))$, $i = 1, 2$ along the turning curve $(C)$ is obtained from (4.2).

$$\begin{aligned} x^P(t_i) &= x^P(t_{i-1}) + (\sin\theta^P(t_i) - \sin\theta^P(t_{i-1}))/\dot{\theta}^P(t), \\ y^P(t_i) &= y^P(t_{i-1}) - (\cos\theta^P(t_i) - \cos\theta^P(t_{i-1}))/\dot{\theta}^P(t), \end{aligned} \tag{4.3}$$

where

$$\dot{\theta}^P(t) = \begin{cases} b & \text{if } \dot{\theta}^P(t) > 0 \\ -b & \text{if } \dot{\theta}^P(t) < 0 \\ 0 & \text{if } \dot{\theta}^P(t) = 0. \end{cases} \tag{4.4}$$

When the pursuer intercepts the stationary target along a straight line $(S)$ at point $(x^P(t_i), y^P(t_i))$, with $i = 3$, it can be expressed as

$$\begin{aligned} x^P(t_i) &= x^P(t_{i-1}) + \cos\theta^P(t_{i-1})(t_i - t_{i-1}), \\ y^P(t_i) &= y^P(t_{i-1}) + \sin\theta^P(t_{i-1})(t_i - t_{i-1}), \end{aligned} \tag{4.5}$$

which yields,

$$\begin{aligned} x^P(t_i) &= x^P(t_{i-1}) + \zeta_i \cos\theta^P(t_{i-1}), \\ y^P(t_i) &= y^P(t_{i-1}) + \zeta_i \sin\theta^P(t_{i-1}), \end{aligned} \tag{4.6}$$

and pursuers heading angles along the straight line ($S$) and curve ($C$) can be found as

$$\theta^P(t_i) = \theta^P(t_{i-1}) + \dot{\theta}^P(t)(t_i - t_{i-1}), \quad i = 1, 2, \tag{4.7}$$

where the left-turn circular arc is represented by $\dot{\theta}^P(t) = b$, the right-turn circular arc by $\dot{\theta}^P(t) = -b$, and the straight line by $\dot{\theta}^P(t) = 0$.
The following equations represents the optimum path $CS$ of the pursuer over the time interval from $t_0$ to $t_3$ using (4.3), (4.4), and (4.6).

$$x^P(t_3) - x^P(t_0) = \frac{1}{b}(-\sin\theta^P(t_0) + 2\sin\theta^P(t_1) - \sin\theta^P(t_2)) + \zeta_3\cos\theta^P(t_2), \tag{4.8}$$

and

$$y^P(t_3) - y^P(t_0) = \frac{1}{b}(\cos\theta^P(t_0) - 2\cos\theta^P(t_1) + \cos\theta^P(t_2)) + \zeta_3\sin\theta^P(t_2). \tag{4.9}$$

It should be noted that when a pursuer intercepts a stationary target, their locations meet up. Stated otherwise, at the point of interception, $(x^P(t_3), y^P(t_3)) = (x^T, y^T)$. Now we write,

$$x^T - x^P(t_0) - \frac{1}{b}(-\sin\theta^P(t_0) + 2\sin\theta^P(t_1) - \sin\theta^P(t_2)) - \zeta_3\cos\theta^P(t_2) = 0, \tag{4.10}$$

and

$$y^T - y^P(t_0) - \frac{1}{b}(\cos\theta^P(t_0) - 2\cos\theta^P(t_1) + \cos\theta^P(t_2)) - \zeta_3\sin\theta^P(t_2) = 0. \tag{4.11}$$

Consequently, the pursuer follows a straight line with the preceding heading angle, $\theta^P(t_2) = \theta^P(t_3)$, after leaving the turning circle.
Hence, we can now create the following mathematical model for intercepting a stationary by taking into account equations (4.7), (4.10), and (4.11).

$$\begin{aligned}
&\min \quad f = \sum_{i=1}^{3}\zeta_i \\
&\text{subject to} \\
&\quad x^T - x^P(t_0) - \frac{1}{b}(-\sin\theta^P(t_0) + 2\sin\theta^P(t_1) - \sin\theta^P(t_2)) - \zeta_3\cos\theta^P(t_2) = 0,, \\
&\quad y^T - y^P(t_0) - \frac{1}{b}(\cos\theta^P(t_0) - 2\cos\theta^P(t_1) + \cos\theta^P(t_2)) - \zeta_3\sin\theta^P(t_2) = 0, \\
&\quad \zeta_i \geq 0, \quad i = 1, 2, 3,
\end{aligned} \tag{4.12}$$

where

$$\theta_1^P = \theta_0^P + b\zeta_1, \quad \theta_2^P = \theta_1^P - b\zeta_2.$$

## 5 Proposed Optimal Path Algorithm

The possible pathways that are described in (4.12) for intersecting a stationary target satisfy the feasible optimal path criteria. We now use mathematical techniques to develop the model that determines the optimal path for the pursuer to take in order to intercept a stationary target that is described as follows.

## 6 Results and Analysis of Numerical Experiments

The numerical experiments of our suggested model (4.12) are presented in this part through multiple numerical experiments. In test problems 1-4, we consider the turning radius of the pursuer turning circle to be one with the unit velocity. As the length of the optimum path differs for different turning radii, we present our model for this situation for the same position of pursuer and target in test problem 5. The efficiency of the algorithm has been evaluated using Test problems 1-5. The results clearly demonstrate the algorithm's effectiveness in calculating pursuer path routes and recommending the best possible trajectory to intercept the target. These are demonstrated in Figures (6.1–6.5) and detailed in Tables (6.1-6.5).
We have used default settings of many solvers, including Ipopt [23] and KNITRO [24], to solve the problems

**Step 1 (Input)**
Set the initial position of the pursuer $P(x_0^P, y_0^P, \theta_0^P)$ and the target at $T(x^T, y^T)$. Set turning radius $R = 1$, curvature $b = \dfrac{1}{R}$. Define the variables for arc length are $\zeta_i$, $i = 1, 2, 3$.

**Step 2 (Determine the trajectory of the pursuers path)**
Let the angle of left turn $\theta^P(t_1) = \theta^P(t_0) + b\zeta_1$,
and angle of right turn $\theta^P(t_2) = \theta^P(t_1) - b\zeta_2$.

**Step 3 (Determine the length of the pursuers initial position to intercept position)**
Set Curve-St.Line := $CS$.
Find $CS := \zeta_1 + \zeta_2 + \zeta_3$ such that
Left turn:
$\zeta_2 = 0$ and $CS := \zeta_1 + \zeta_3$,
Or
Right Turn:
$\zeta_1 = 0$ and $CS := \zeta_2 + \zeta_3$.

**Step 4 (Find total optimum length)**
Find $\zeta := (\zeta_1, \zeta_2, \zeta_3)$ that solves model (4.12) and $f = \sum_{i=1}^{3} \zeta_i$.

in the tests. We have implemented Algorithm (1) writing programs in AMPL [25]. In addressing our problem, nearly every solution demonstrated a high rate of convergence. MATLAB is used to simulate the acquired solutions in the numerical experiments as test problems. To simulate our experimental results we use HP ProBook 440 G6 laptop with 8GB RAM and 4.6 GHz Core i7 processor.

**Test Problem 1**

We considered that the initial position of the pursuer is $P(0, 0, 2\pi/3)$ and fix the target at $T(10, 5)$. Assuming the turning radius is one for the turning curve of the pursuer. After testing the model (4.12) we observed that the pursuer takes the right turn to find the optimum path and takes a turn left for the feasible path. The total optimum length found by the test is 11.87 with the solving time 0.031 seconds, while the feasible length is 16.88 by AMPL is taken approximately 0.047 seconds. The comparable path results of the optimum and feasible path are shown in Table (6.1) and the figure of both possible paths is demonstrated in Figure (6.1)

Table 6.1: *Experimental Solutions for Optimum and Feasible Path generations*

| Positions | Length | | | |
|---|---|---|---|---|
| $P(0, 0, 2\pi/3)$ $T(10, 5)$ $R = 1$ | Left turn $\zeta_1$ | Right turn $\zeta_2$ | St. line $\zeta_3$ | Total value $f$ |
| Optimal Path | 0 | 1.74 | 10.13 | 11.87 |
| Feasible Path | 4.74 | 0 | 12.14 | 16.88 |

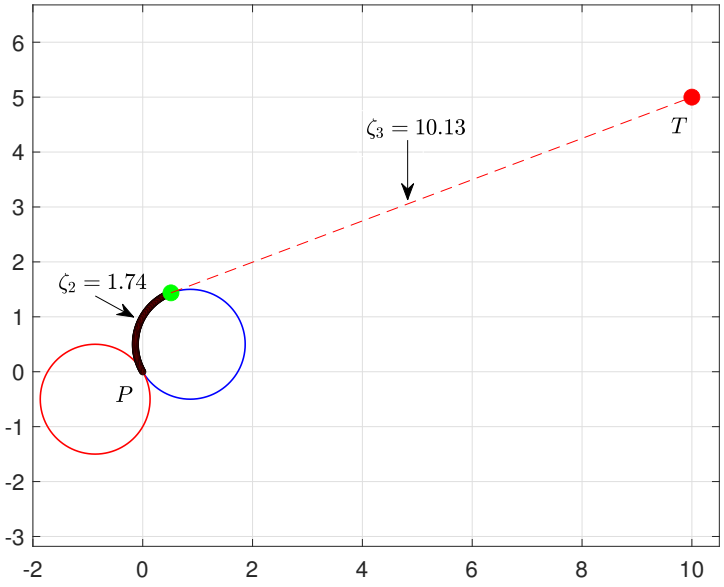


(a) Optimal path.

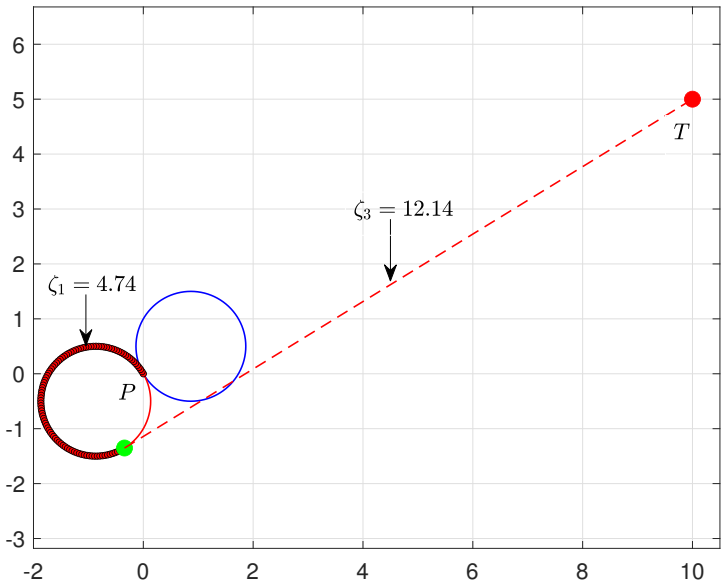


(b) Feasible path.

Figure 6.1: Interception path of the pursuer position $P(0,0)$ with a heading angle of $\theta^P = 2\pi/3$ and target $T(10,5)$.

**Test Problem 2**

Now we assume the target position is left side of the pursuer. Let the initial position of the pursuer is $P(0,0,2\pi/3)$ and the target at $T(-6,3)$. Assuming the pursuer moves with a turning radius of one. After testing the model (4.12) we observed that the pursuer takes a left turn to find the optimum path and takes a turn right for the feasible path. The total optimum length found by the test is 6.74 with the solve time 0.047 seconds while the feasible length is 12.96 by AMPL is taken approximately 0.016 seconds. The comparable path results of the optimum and feasible path are shown in Table (6.2) and the figure of both possible paths is demonstrated in Figure (6.2).

Table 6.2: *Experimental Solutions for Optimum and Feasible Path generations*

| Positions | Length | | | |
|---|---|---|---|---|
| $P(0,0,2\pi/3)$ $T(-6,3)$ $R = 1$ | Left turn $\zeta_1$ | Right turn $\zeta_2$ | St. line $\zeta_3$ | Total value $f$ |
| Optimal Path | 0.61 | 0 | 6.13 | 6.74 |
| Feasible Path | 0 | 5.72 | 7.24 | 12.96 |

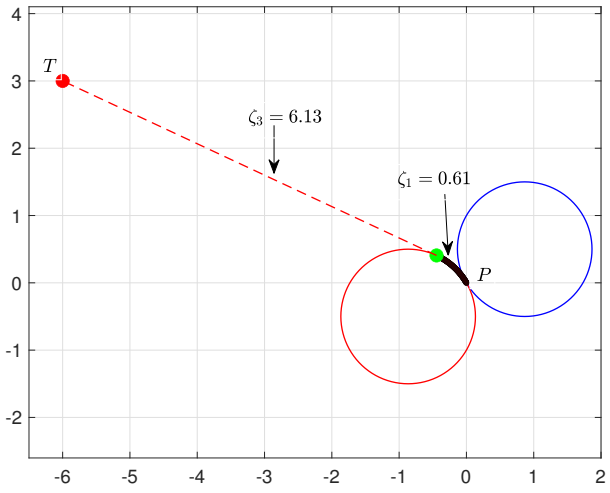


(a) Optimal path.

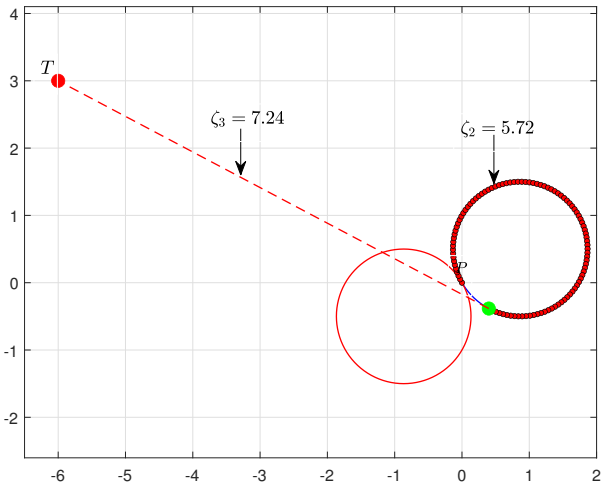


(b) Feasible path.

Figure 6.2: Interception path of the pursuer position $P(0,0)$ with a heading angle of $\theta^P = 2\pi/3$ and target $T(-6,3)$.

**Test Problem 3**

In this problem we fixed the target position is upside of the pursuer. Let the target position be at $T(-1,5)$. Assuming the pursuer moves from $P(0,0)$ with heading angle $\pi/3$ along a turning radius one. Now we observed that the pursuer takes a left turn to find the optimum path and takes a turn right for the feasible path. The

total optimum length found by the test is 5.17 with the solving time 0.016 seconds while the feasible length is 11.33 by AMPL is taken approximately 0.031 seconds. The comparable path results of the optimum and feasible path are shown in Table (6.3) and the figure of both possible paths is demonstrated in Figure (6.3).

Table 6.3: *Experimental Solutions for Optimum and Feasible Path generations*

| Positions | Length | | | |
|---|---|---|---|---|
| $P(0,0,\pi/3)$ $T(-1,5)$ $R = 1$ | Left turn $\zeta_1$ | Right turn $\zeta_2$ | St. line $\zeta_3$ | Total value $f$ |
| Optimal Path | 0.79 | 0 | 4.39 | 5.17 |
| Feasible Path | 0 | 5.61 | 5.72 | 11.33 |

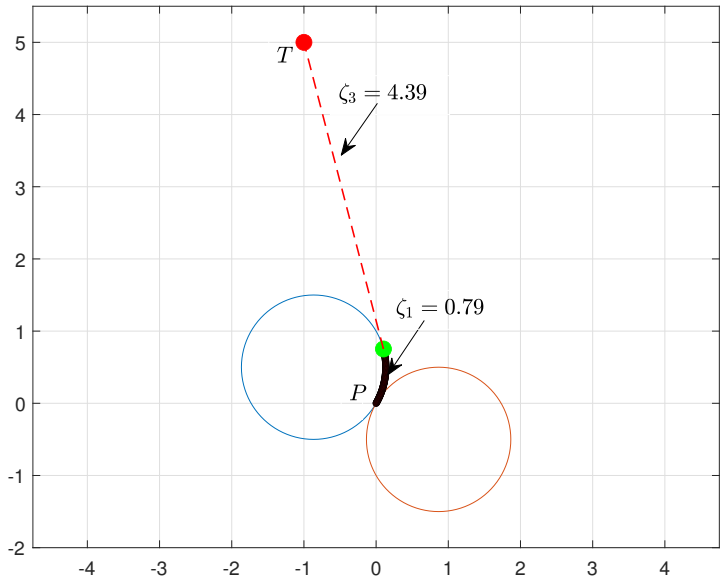


(a) Optimal path.

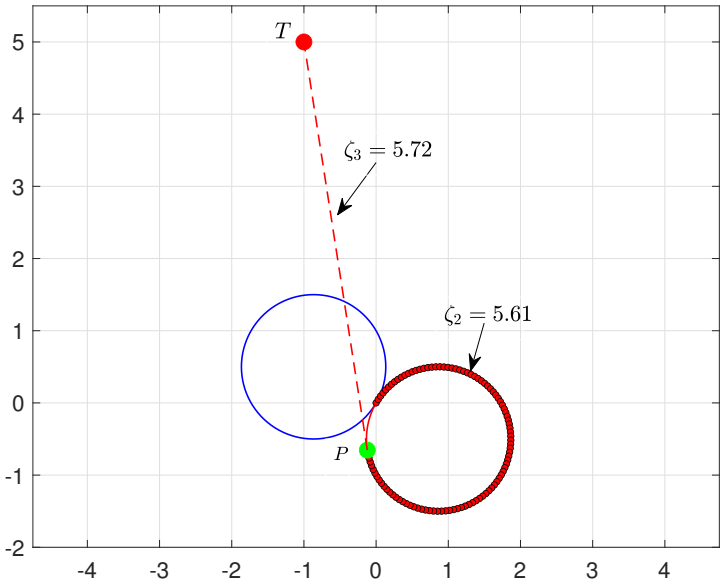


(b) Feasible path.

Figure 6.3: Interception path of the pursuer position $P(0,0)$ with a heading angle of $\theta^P = \pi/3$ and target $T(-1,5)$.

### Test Problem 4

Now we locate the target is another location which is below the pursuer position. Assume the target position be at $T(-2,-5)$. Assuming the pursuer moves from $P(0,0)$ with heading angle $\pi/3$ along a turning radius one. After testing the problem we find that the pursuer takes a right turn to find the optimum path and takes a left right for the feasible path to intercept the target. The total optimum length in the interception found by the test is 8.61 with the solving time 0.031 seconds while the feasible path length is 9.17 by AMPL is taken approximately 0.047 seconds. The comparable path results of the optimum and feasible path are shown in Table (6.4) and the figure of both possible paths is demonstrated in Figure (6.4).

Table 6.4: *Experimental Solutions for Optimum and Feasible Path generations*

| Positions | Length | | | |
|---|---|---|---|---|
| $P(0,0,\pi/3)$ $T(-2,-5)$ $R = 1$ | Left turn $\zeta_1$ | Right turn $\zeta_2$ | St. line $\zeta_3$ | Total value $f$ |
| Optimal Path | 0 | 3.38 | 5.24 | 8.61 |
| Feasible Path | 3.64 | 0 | 5.53 | 9.17 |

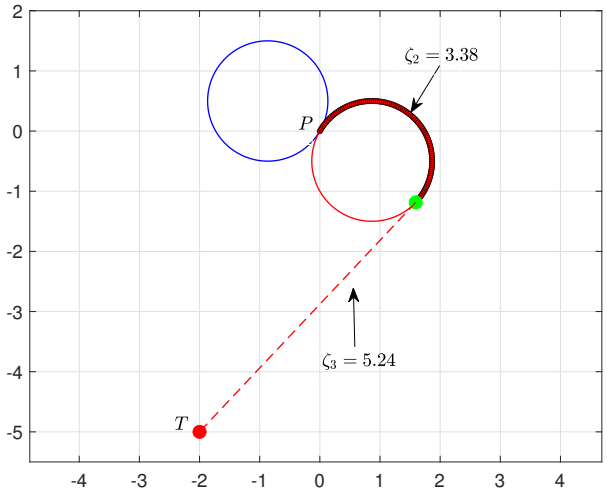


(a) Optimal path.

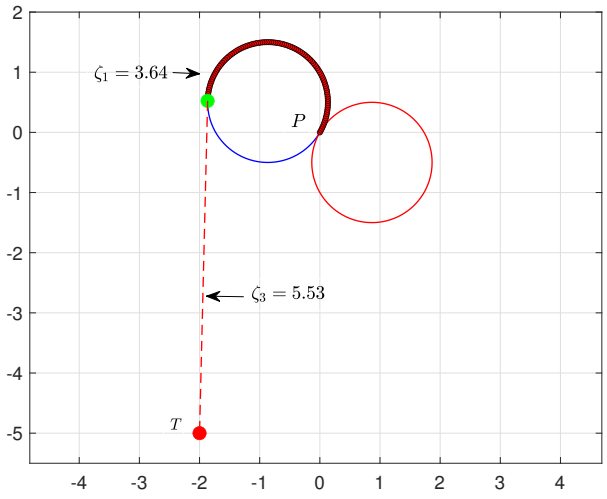


(b) Feasible path.

Figure 6.4: Interception path of the pursuer position $P(0,0)$ with a heading angle of $\theta^P = \pi/3$ and target $T(-2,-5)$.

**Test Problem 5**

In this problem, we show that how can effect the variation of turning radius on the path length. We demonstrate our model for three different turning radii of the pursuer turning curve while the initial position and the target position remain constant. Let the initial position of the pursuer is $P(0, 0, 2\pi/3)$ and the target position be at $T(-80, 20)$. First, we take the pursuer turning radius is 10. After performing our model (4.12), we find that the pursuer takes a left turn to find the optimum path and takes a right turn for the feasible path to intercept the target. The total optimum length in the interception found by the test is 83.36 with the solve time 0.047 seconds.Again we test the same problem with another two turning radius 5 and 25. The comparable path results for different turning radii are shown in Table (6.5) and the figure of both possible paths is demonstrated in Figure (6.5).

Table 6.5: *Experimental Solutions for Different Turning Radii*

| Positions | Length | | | |
|---|---|---|---|---|
| $P(0, 0, 2\pi/3)$ $T(-80, 20)$ $R = 1/\lvert\dot{\theta}(t)\rvert$ | Left turn $\zeta_1$ | Right turn $\zeta_2$ | St. line $\zeta_3$ | Total value $f$ |
| $R = 25$ | 23.01 | 0 | 61.91 | 84.92 |
| $R = 10$ | 8.43 | 0 | 74.92 | 83.36 |
| $R = 5$ | 4.11 | 0 | 78.79 | 82.89 |

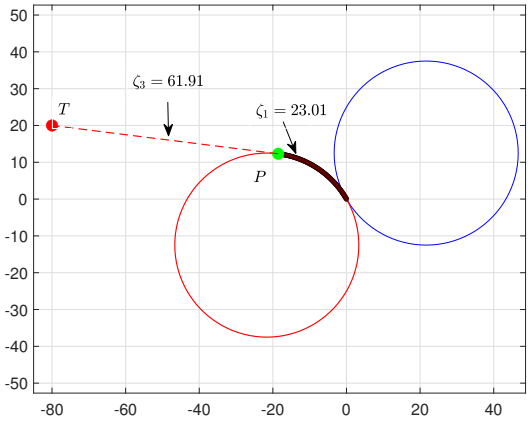


(a) Optimal path when $R = 25$

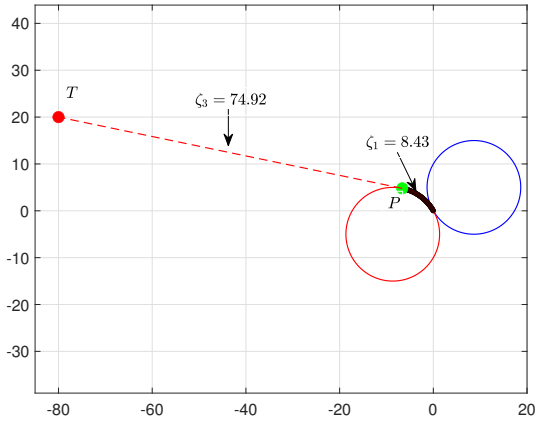


(b) Optimal path when $R = 10$

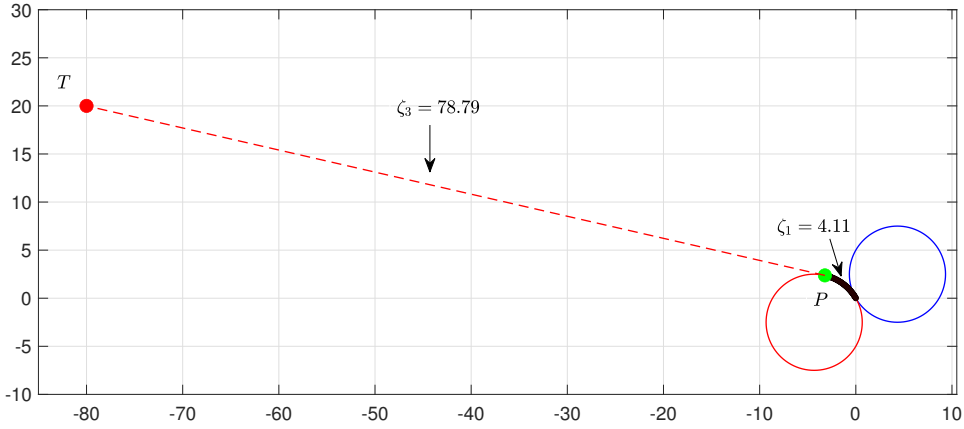


(c) Optimal path when $R = 5$.

Figure 6.5: Interception path of the pursuer position $P(0, 0)$ with a heading angle of $\theta^P = 2\pi/3$ and target $T(-80, 20)$.

The model provides solutions for both Dubin path LS (Left turn and straight) and RS (Right turn and straight), as discussed in the geometric principles (3.1). Additionally, it is important to note that the heading angle of the pursuer's movement ranges within the interval of $0 \leq \theta^P \leq 2\pi$. Within this range, the model has been extensively tested and verified through various test problems (specifically, Test Problems 1-5). The efficiency of the solutions within this specified interval has been thoroughly justified.

# 7 Conclusion

In this paper, our research offered a reliable and effective method for finding the shortest route for a pursuer to intercept a stationary target. The proposed mathematical model integrated segments of straight lines and circular curves using the ideas of Dubin's path to minimise the lengths of the pursuer's path. We tested our model in various positions of the target and pursuer with different heading angles. We observed a significant rate of convergence to approximate solutions of the proposed model. In summary, the mathematical model serves to optimize path planning for unmanned aerial vehicles (UAV), addressing key challenges in dynamic environments and advancing the capabilities of autonomous vehicles. The developed model opens avenues for further research and development in pursuit of optimal path-planning solutions in dynamic and complex environments.

**Acknowledgments:** The author, M. Akter, would like to thank the Ministry of Science and Technology, Bangladesh, for the financial assistance she received as an NST fellow (Reference no. 120005100-3821117, Reg. no. 6 & Session: 2022–2023).
Additionally, we thank Chatgpt(3.5) for its artificial intelligence technologies, which are utilized to reword, edit, and polish writers' writing for proper grammar, spelling, and style.

## References

[1] Dubins, L. E., On curves of minimal length with a constraint on average curvature, and with prescribed initial and terminal positions and tangents. American Journal of mathematics, 79(3), 497-516, (1957).

[2] Boissonnat, J. D., Cerezo, A., Leblond, J., Shortest paths of bounded curvature in the plane. Journal of Intelligent and Robotic Systems, 11, 5-20, (1994).

[3] Bui, X. N., Boissonnat, J. D., Soueres, P., Laumond, J. P., Shortest path synthesis for Dubins non-holonomic robot. In Proceedings of the 1994 IEEE International Conference on Robotics and Automation, 2-7, (1994).

[4] Chitsaz, H., LaValle, S. M., Time-optimal paths for a Dubins airplane. In 2007 46th IEEE conference on decision and control, 2379-2384, (2007).

[5] Jha, B., Chen, Z., Shima, T., On shortest Dubins path via a circular boundary. Automatica, 121, 109192, (2020).

[6] Manyam, S. G., Casbeer, D., Von Moll, A., Fuchs, Z., Optimal dubins paths to intercept a moving target on a circle. In 2019 American Control Conference (ACC), 828-834, (2019).

[7] Sussmann, H. J., Tang, G., Shortest paths for the Reeds-Shepp car: a worked out example of the use of geometric techniques in nonlinear optimal control. Rutgers Center for Systems and Control Technical Report, 10, 1-71, (1991).

[8] Ayala, J., Kirszenblat, D., & Rubinstein, H., A Geometric approach to shortest bounded curvature paths. Communications in Analysis and Geometry, 26(4), 679-697, (2018).

[9] Manyam, S. G., Casbeer, D., Von Moll, A. L., Fuchs, Z., Shortest Dubins path to a circle. In AIAA scitech 2019 forum, 919, (2019).

[10] Chen, Z., Shima, T., Shortest Dubins paths through three points. Automatica, 105, 368-375, (2019).

[11] Chen, Z., On Dubins paths to a circle. Automatica, 117, 108996, (2020).

[12] Stone, L. D., Theory of Optimal Search, 2-nd ed. Operations Research Society of America, Arlington, VA, 38, 415-422, (1989).

[13] Zadka, B., Tripathy, T., Tsalik, R., Shima, T., Consensus-based cooperative geometrical rules for simultaneous target interception. Journal of Guidance, Control, and Dynamics, 43(12), 2425-2432, (2020).

[14] Chen, Z., Shima, T., Nonlinear optimal guidance for intercepting a stationary target. Journal of Guidance, Control, and Dynamics, 42(11), 2418-2431, (2019).

[15] Hough, M. E., Optimal guidance and nonlinear estimation for interception of decelerating targets. Journal of Guidance, Control, and Dynamics, 18(2), 316-324, (1995).

[16] Zhou, J., Yang, J., Li, Z., Simultaneous attack of a stationary target using multiple missiles: a consensus-based approach. Science China Information Sciences, 60, 1-14, (2017).

[17] Looker, J. R., Minimum Paths to Interception of a Moving Target when Constrained by Turning Radius, (2008).

[18] Kaya, C. Y., Markov–Dubins path via optimal control theory. Computational Optimization and Applications, 68(3), 719-747, (2017).

[19] Kaya, C. Y., Markov–Dubins interpolating curves. Computational Optimization and Applications, 73(2), 647-677, (2019).

[20] Zheng, Y., Chen, Z., Shao, X., & Zhao, W., Time-optimal guidance for intercepting moving targets by dubins vehicles. Automatica, 128, 109557, (2021).

[21] Forkan, M., Rizvi, M. M., Chowdhury, M. A. M., Optimal path planning of Unmanned Aerial Vehicles (UAVs) for targets touring: Geometric and arc parameterization approaches. Plos one, 17(10), e0276105, (2022).

[22] Pontryagin, L. S., Boltyanskii, V.G, Gamkrelidze, R. V., Mishchenko, E. F., The mathematical theory of optimal processes (Russian), John Wiley and Sons, Interscience Publishers, New York, (1962).

[23] Wächter, A., and Biegler, L. T., On the implementation of an interior-point filter line-search algorithm for large-scale nonlinear programming. Mathematical programming, 106, 25-57, (2006).

[24] Byrd, R. H., Nocedal, J., Waltz, R. A., Knitro: An integrated package for nonlinear optimization. Large-scale nonlinear optimization, 35-59, (2006).

[25] Fourer, R., Gay, D. M., Kernighan, B. W., AMPL: A Modeling Language for Mathematical Programming, Second Edition, Brooks/Cole Publishing Company / Cengage Learning, (2003).